JMBFS
Journal of Microbiology, Biotechnology and Food Sciences
International peer-reviewed scientific online journal

Published by Faculty of Biotechnology and Food Sciences

SYNTHESIS, CHARACTERIZATION, ANTIMICROBIAL AND ELECTROCHEMICAL STUDIES OF BIOSYNTHESIZED ZINC OXIDE NANOPARTICLES USING THE PROBIOTIC *BACILLUS COAGULANS* (ATCC 7050)

Rolla M. Fayed[1], *Abdel-Menem Elnemr*[2], *Mohamed M. El-Zahed*[1]*

Address(es):
[1] Damietta University, Faculty of Science, Department of Botany and Microbiology, New Damietta, Egypt.
[2] Damietta University, Faculty of Science, Department of Physics, New Damietta, Egypt.

*Corresponding author: mohamed.marzouq91@du.edu.eg

https://doi.org/10.55251/jmbfs.9962

ARTICLE INFO

Received 8. 3. 2023
Revised 4. 7. 2023
Accepted 31. 7. 2023
Published 1. 12. 2023

Regular article

OPEN ACCESS

ABSTRACT

Nowadays, nanotechnology has been used to overcome many global problems such as growing worldwide demand for energy and problems of microbial antibiotic resistance. The presented study used the probiotic *Bacillus coagulans* (ATCC 7050) as a nano-factory for the biosynthesis of zinc oxide nanoparticles (ZnO NPs). UV-visible spectroscopy, FTIR spectroscopy, XRD, TEM and Zeta analysis confirmed the formation of spherical ZnO NPs with a mean size of 10-19 nm and positive potential of 29±2 mV. The biosynthesized ZnO NPs showed potent antimicrobial activity against Gram-positive and Gram-negative bacteria as well as pathogenic yeast with minimum inhibition concentration (MIC) values of 500 and 800 µg/ml against *Staphylococcus aureus* ATCC 25923 and *Pseudomonas aeruginosa* ATCC 27853 and 600 µg/ml against *Candida albicans* ATCC 10231. On the other hand, a voltaic cell composed from an immersed reduced copper (positive electrode) and platinum electrodes (negative electrode) in ZnO NPs/bacterial metabolites was connected to a voltameter and used to study the electrochemical activity of ZnO NPs/*B. coagulans* metabolites. Electrochemical characterization of ZnO NPs/*B. coagulans* metabolites was done using current density–voltage characteristic, power density and electrochemical impedance spectroscopy (EIS) analyses. ZnO NPs/*B. coagulans* metabolites produced high current with voltage value ≈ >0.34 volt. The present study reported the ability of *B. coagulans* to produce nitrate reductase enzyme with enzyme activity 2.18 U/ml. The reduction pathway of nitrate (NO_3^-) into nitrite (NO_2^-) during the biosynthesis of ZnO NPs might help and stimulate the current production.

Keywords: Zinc oxide, nanoparticles, *Bacillus coagulans*, antimicrobial activity, electrochemical activity

INTRODUCTION

Antimicrobial agents have two different effects on the bacterial cells either bactericidal or bacteriostatic action. However, many bacterial strains acquired a resistance against different current traditional antimicrobial agents due to the misuse and overuse of multiple antimicrobial agents throughout several industries including packaging, paints, food, building, water treatment moreover their applications in the healthcare and biomedical fields **(Griffith et al., 2022; Hazra et al., 2022)**. This phenomenon increased and became great problematic which made disease treatment more complex and increased death rate. Thus, the development of innovative antimicrobial agents to address the persistent evolution of pathogens had a great attention in last decades.

Lately, nanotechnology has developed as a safe and effective technology to overcome this problem. Nanomaterials (1 to100 nm) are an exceptional class of materials that have various distinctive physicochemical and biological properties compared to their bulks with larger scales **(El-Zahed et al., 2022a; Raval et al., 2022; Zhao et al., 2020)**. There are different chemical and physical methods used for the synthesis of nanomaterials including Sol-Gel method, thermal decomposition, chemical vapor deposition, laser ablation and microwave synthesis **(Khan, 2020; Rajput, 2015)**. But the synthesized nanomaterials were found to have cytotoxicity effects on human cells, which could have negative effects in medicinal applications. Alternatively, biological methods that uses plants and different microbes during the biosynthesis process produced biocompatible, stable, and non-toxic nanomaterials **(Raina et al., 2020)**. Nano-metal oxides such as ZnO, AgO and CuO are one of the most recent nanomaterials that revealed strong antimicrobial action against different pathogenic bacteria such as *Escherichia coli*, *Pseudomonas aeruginosa*, *Klebsiella pneumoniae*, *Staphylococcus aureus* and *Enterococcus faecalis* **(Dizaj et al., 2014; Jagadeeshan & Parsanathan, 2019)**, pathogenic fungi such as *Aspergillus niger*, *Fusarium oxysporum* and *Alternaria solani* **(Azimirad & Safa, 2014; Yu et al., 2013)** as well as pathogenic yeasts such as *Candida albicans* and *C. glabrata* **(El-Nahhal et al., 2017; Karimiyan et al., 2015)**. Among nanometal oxides, ZnO showed no mortality and no toxicity against normal human cell lines **(Alarifi et al., 2013)**. Many studies recorded the biosynthesis of zinc oxide nanoparticles (ZnO NPs) using different bacterial strains such as *B. foraminis* **(EL-Ghwas, 2022)**, *B. subtilis* ZBP4 **(Hamk et al., 2022)** and *Lactobacillus plantarum* TA4 **(Mohd Yusof et al., 2020)**.

On the other hands, a very real energy crisis is currently being caused by the rising worldwide demand for energy, the issues of scarcity and the environmental impact of existing sources. Petroleum will become more expensive and scarcer, and by that time, the negative effects of extensive usage of all fossil fuels on the climate will be clear. The unregulated and excessive use of current energy resources over the past few decades has contributed to the depletion of traditional resource types. In addition, these fossil fuels caused numerous diseases for human, animals, and plants **(Lisha et al., 2023)**. So, scientists compete to find alternative safe and eco-friendly energy sources. Electrical energy is one of the most reliable, effective, and efficient generation of energy. Over the next few decades, renewable electricity is considered the most important challenge and will be enormously increasing the influence of renewable energy compared to existing levels. Different biological systems such as algae, fungi, and bacteria were used as a natural source of energy. The biomass from biological systems was applied in several purposes, including cooking, heating, industries, and energy **(Lisha et al., 2023)**. Bacteria was reported as electrically carrying microorganisms throughout getting rid of the electrons that make when they produce energy **(Lovley & Phillips, 1988; Malvankar et al., 2011)**.

The unique physical and chemical properties of ZnO NPs, such as their high chemical stability, strong electrochemical coupling coefficient, broad spectrum of radiation absorption, paramagnetic nature, and high photostability, make them a versatile material **(Parihar et al., 2018)**. Regarding the employment of hazardous bacteria, this is an alternate method of generating energy as a source of sustainable energy. As an illustration, some solar cells contain toxic materials **(Mariotti et al., 2020)**. This energy is supplied from renewable resources and is not dependent on fossil fuels. Because of their distinct optical, electrical, and electrochemical properties, ZnO NPs have received much research in electrochemical applications **(Faizan et al., 2021)**. ZnO NPs have been investigated as electrode materials for electrochemical sensing and energy storage devices such as batteries and supercapacitors. ZnO NPs can be utilised as an electrode material in electrochemical sensing to find diverse analytes, like gases, biomolecules, and heavy metals. ZnO nanoparticles are a good candidate for sensitive and selective electrochemical sensing applications due to their large surface area and distinctive electrical characteristics **(Thareja & Kumar, 2021)**. Due to its great cycling stability and high specific capacity, ZnO NPs have been employed as an electrode material for lithium-ion batteries in energy storage systems. Because of their great

electrical conductivity and high surface area, they have also been employed as a component in supercapacitors **(Zhang et al., 2017)**.
The present study aimed to use the probiotic *Bacillus coagulans* (ATCC 7050) as a new electrically carrying microorganisms to produce renewable and available alternative source of electrical energy as -to our knowledge- a first record in addition to extracellular biosynthesize of antimicrobial ZnO NPs and further subjected to characterization and evaluation of antimicrobial action against different pathogens.

MATERIALS AND METHODS

Extracellular biosynthesis of ZnO NPs

Lyophilized culture of *Bacillus coagulans* (ATCC 7050) was obtained from the Microbiology Laboratory, Faculty of Science, Damietta University (Damietta, Egypt), subcultured for 24 hr at 37°C on de Man, Rogosa and Sharp (MRS, Oxoid) agar plates and reactivated three times before use. After incubation time, 3 single colonies were inoculated aerobically in a nutrient broth medium (Oxoid) and incubated at 37°C and 150 rpm for 24 hr. Bacterial supernatants were collected by centrifugation at 5000 rpm for 15 min under aseptic conditions. Then, cell-free supernatants were obtained by passing the supernatants through millipore filters. 20 ml of cell-free supernatant was mixed with 100 ml of zinc sulphate ($ZnSO_4$, Sigma Aldrich, ACS reagent, 99%) solution (3 mM) and stirred for 24 hr at room temperature (25°C) and dark conditions. The biosynthesis of ZnO NPs was observed via the visible colour change and light-yellow precipitate formation. Mixtures were centrifugation centrifugated at 8000 rpm for 15 min to collect ZnO NPs precipitate and dried at 80 °C. The precipitate was dried completely and calcined at 400°C for 2 hr **(Rajabairavi et al., 2017)**.

Characterization of the biosynthesized ZnO NPs

The biosynthesis of ZnO NPs was examined spectrophotometrically (Beckman DU-40) and using Fourier transform infrared spectroscopy (FTIR, FT/IR-4100typeA). The X-ray diffraction pattern (XRD), Zeta potential and transmission electron microscopic (TEM) analyses for ZnO NPs were also recorded with an X-ray diffractometer (model LabX XRD-6000, Shimadzu, Japan), TEM apparatus (200 kV, TEM JEOL JEM-2100, Japan) and Zeta potential analyser (Malvern Zetasizer Nano-ZS90, Malvern, UK).

Evaluation of antimicrobial activity of biosynthesized ZnO NPs

Agar well diffusion method

The antimicrobial actions of ZnO NPs were tested against different microbial models, obtained from the Microbiology Laboratory, Faculty of Science, Damietta University (Egypt), including Gram-positive bacterium (*S. aureus* ATCC 25923), Gram-negative bacterium (*Pseudomonas aeruginosa* ATCC 27853) and a pathogenic yeast (*Candida albicans* ATCC 10231) **(Clinical and Laboratory Standards, 2017)**. Different concentrations (1000, 3000 and 5000 µg/ml) of ZnO NPs, $ZnSO_4$, and penicillin or fluconazole (Sigma-Aldrich, as standard antibiotics) were prepared, dissolved in dimethyl sulfoxide (DMSO), and added (100 µl) into wells (5mm) in Mueller-Hinton (MHA) or Sabouraud dextrose (SDA) agar media (Oxoid) plates inoculated by10^8 or 10^6 CFUs/ml from bacteria or yeast, respectively. The agar plates were incubation at 37°C for 48 hr. After incubation period, zones of inhibition (ZOI) were calculated in millimetres (mm).

Minimum inhibition concentration (MIC) and minimum microbicidal concentration (MBC)

MIC and MBC for the biosynthesized ZnO NPs were studied using the broth dilution method **(Clinical and Laboratory Standards, 2000)**. Aliquot 50 ml of Mueller-Hinton or Sabouraud dextrose broth media (Oxoid) supplemented with 100-1000 µg/ml ZnO NPs, penicillin or fluconazole were inoculated with 100 µl of overnight bacterial (10^8 CFU/ml) or yeast culture (10^6 CFU/ml), respectively, and incubated at 37°C and 150 rpm for 24 hr. MIC of the ZnO NPs (no apparent growth) was determined spectrophotometrically at 600 nm. To determine the MBC, aliquot 10 µl of each set was inoculated on MHA or SDA plate for bacteria or yeast culture, respectively, and incubated at 37°C for 24 hr. The MBC of the ZnO NPs (no apparent growth plates) was recorded.

Ultrastructure study

The antibacterial action of the ZnO NPs was investigated using *P. aeruginosa* as a model organism. Centrifugation was used to separate untreated and ZnO NPs-treated bacteria with MIC values from 24 hr old cultures grown on nutrient broth media. After being fixed for three minutes in phosphate buffer solution and 5 min in potassium permanganate solution, the bacterial pellets were washed with 3% glutaraldehyde. The fixed samples were dehydrated for 15 min in a series of ethanol dilutions ranging from 10 to 90%, and then for 30 min in pure ethyl alcohol. The samples were filtrated with epoxy resin and acetone through a graded series till finally in pure resin. Ultrathin sections were collected on copper grids, then stained. The stained sections were observed with a TEM JEOL JEM-2100, Japan **(El-Dein et al., 2021)**.

Electrode preparation

Voltaic cell composed of an emersed reduced copper electrode in cell-free supernatants of ZnO NPs/*B. coagulans* (ATCC 7050) as a positive electrode in addition to a platinum electrode as a negative electrode that connected to voltammeter (µA) was prepared and used for measuring the produced voltage (Figure 1). Also, cell-free supernatants of ZnO NPs/*B. coagulans* was tested to light a led lamp in the voltaic cell connected to a LED lamp instead of the voltmeter.

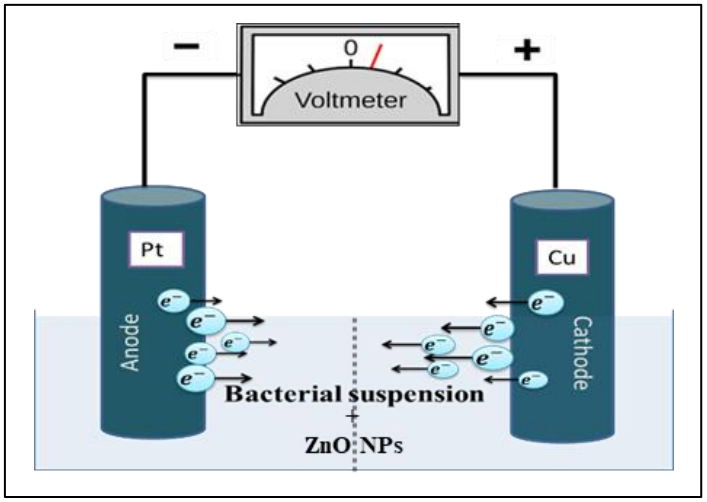

Figure 1 Diagram of testing the voltage production using cell-free supernatant of ZnO NPs/*B. coagulans* (ATCC 7050).

Electrochemical analyses of cell-free supernatants of ZnO NPs/*B. coagulans*

Current density–voltage characteristic and power density cell-free supernatants of ZnO NPs/*B. coagulans* were measured by Metrohm Autloab (PGSTAT204) Nova2 software. Then, electrochemical impedance spectroscopy (EIS) analysis of the fabricated DSSC employing samples was carried out between 0.1 Hz and 100 kHz at an open-circuit AC potential of 10 mV using a frequency response analyzer and fitted to an equivalent circuit model using the Metrohm Autloab (PGSTAT204) Nova2 software (Optoelectronics Lab, Physics Department, Faculty of Science, Damietta University, Egypt).

Total protein estimation and NADH dependent enzymes assay

Total protein content of *B. coagulans* (ATCC 7050) was estimated by Bradford method **(Bradford, 1976)**. Nitrate reductase (NR) activity was measured spectrophotometrically at 540 nm according to **Harley (1993)** depending on the reduction of nitrate into nitrite as a model for NADH dependent reductase enzyme. Nitrite standard curve was prepared and used to calculate the amount produced by enzyme activity. Production of one µmol nitrite/h/ml was defined as one unit of NR activity (U/ml).

Statistical analysis

SPSS software version 18 was used to analyse results using the ANOVA test. The threshold for significance was fixed at 0.05. The experiments were carried out three times. All values were reported as the mean and standard error (SE) **(O'connor, 2000)**.

RESULTS AND DISCUSSION

People take *B. coagulans* for irritable bowel syndrome (IBS), diarrhea, gas, airway interpret, and many other conditions, but there is no good scientific evidence to support these uses **(Liu et al., 2018)**. The bacteria that cause gangrene (*Clostridium perfringens*) and hospital-acquired infections (*Enterococcus faecalis*) and some disease-causing streptococcus bacteria were used to produce electricity **(Mukhaifi & Abduljaleel, 2020)**. On the other hand, the presented study used *B. coagulans*, similarly to *Lactobacillus* sp. and other probiotics as "beneficial" bacteria, to biosynthesize ZnO NPs with potent antimicrobial activity and studied their electrochemical behaviour.

Biosynthesis and characterization of ZnO NPs

Many studies had documented the ability of bacteria to biosynthesize different NPs via several mechanisms **(Pandit et al., 2022)**. One of the recommended pathway for NPs biosynthesis at dark conditions is the bioreduction of metal ions using NADH dependent enzymes into nanometals or nanometal oxides **(Yusof et al., 2019)**. This biosynthesis method may occur either intracellularly or extracellularly **(Mahdi et al., 2021)**. However, the extracellular methods are more favourable due to the intracellular methods requires extra-steps such as cell breakdown, extraction and purification of the produced **NPs (Mahdi et al., 2021)**. *B. coagulans* (ATCC 7050) could biosynthesize ZnO NPs extracellularly within 24 hr at room temperature (25°C) and dark conditions.

ZnO NPs formation was confirmed and characterized by different techniques. The colour change into pale yellow indicated to the biotransformation of zinc ions in the presence of *B. coagulans* cell-free supernatant to ZnO NPs which assigned to excitation of ZnO NPs surface plasmon resonance (SPR) **(Rehman et al., 2019)**. The UV-visible spectrometer absorption peak was appeared at 318 nm, which is specific for ZnO NPs (Figure 2A). This absorption peak agree well with the ZnO NPs absorption band reported by **(Mousa & Khairy, 2020)**. On the other hand, **Rehman et al. (2019)** applied *B. haynesii* for the biosynthesis of ZnO NPs which showed a broad absorption with peak maxima at about 350 nm.

FTIR spectrum of ZnO NPs was measured from 400 to 4000 cm^{-1} and confirmed the presence of proteins in the biosynthesis of nanoparticles. (Figure 2B). During the bioformation of ZnO NPs, absorption peaks in *B. coagulans* crude metabolites at 3271.6, 1457.3, 1295.3, and 919 cm^{-1} were shifted into 3390.4, 1645.1, 1349.3, and 1072.3 cm^{-1}. Stretching vibrations of metal-oxygen appeared between 400–600 cm^{-1} indicating to the presence of ZnO **(Lai et al., 2011)**. The hydroxyl groups stretching appeared as broad peaks at 3390.4, 3271.6 cm^{-1}. The secondary amines vibration band located at 2929.5 and 2860 cm^{-1}. Vinyl and cis-tri substituted absorption peaks raised at 1645.1 cm^{-1}. Amines stretching vibrations appeared at 1457.3, 1259.3 and 1394.3 cm^{-1}. The carbon–oxygen bond stretching located at 1072.3 cm^{-1} while carbon–hydrogen bond stretching presented at 881.5 and 781.1 cm^{-1}.

XRD of ZnO NPs was analysed between 10° and 80° of 2θ range (Figure 2C). ZnO crystalline peaks appeared at 32.3°, 35.2°, 36.6°, 57.2°, 64.3° and 67.2° corresponding to the lattice planes (100), (002), (101), (110), (103) and (112) that matched with results. Debye-Scherrer equation ($D = k\lambda/\beta cos\theta$; where D; average crystalline particle size, λ; wavelength of x-ray (1.5406 Å), k; Scherer's constant (0.9), θ; diffraction angle, and β; XRD peak full width at half maximum) was applied to calculate ZnO NPs size. The average size was found to be 17±1.5 nm which matched with the TEM results. According to several studies, the effectiveness of antibacterial activity of nanoscaled particles depends on the size of the particles **(El-Dein et al., 2021; Khurana et al., 2014; Shivashankarappa & Sanjay, 2015)**. Smaller particles have a more potent antibacterial effect than larger ones and may negatively impact microbial protoplasts by causing DNA molecules to condense, inhibiting replication, deactivating enzymes and metabolism, and causing membrane permeability to malfunction **(Gold et al., 2018)**. Small particles may also have an adverse effect on microbial cell walls and cytoplasmic membranes **(Yin et al., 2020)**.

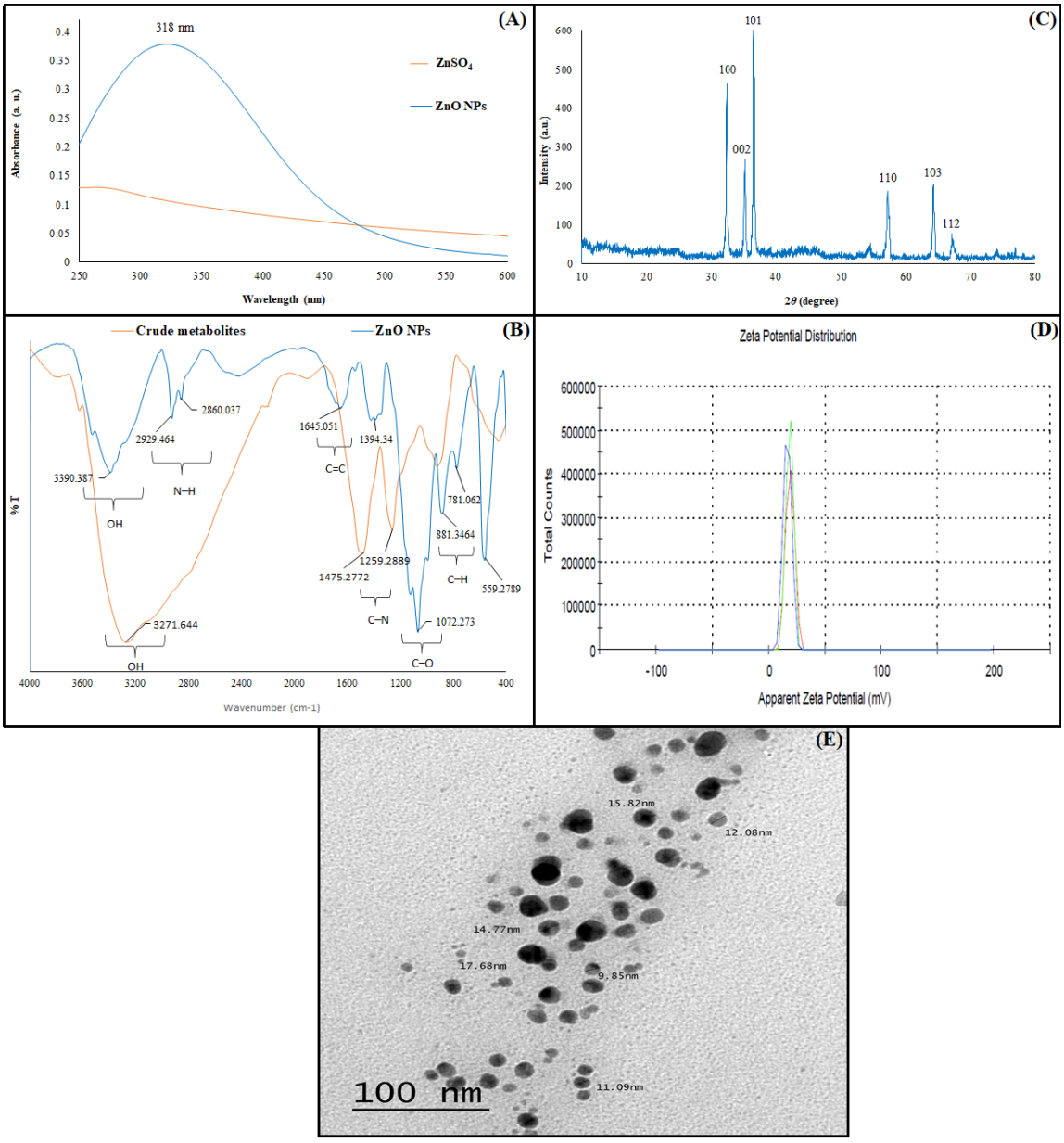

Figure 2 Characterization of the biosynthesized ZnO NPs. (A) UV-visible spectroscopy of ZnO NPs in comparing to $ZnSO_4$. (B) FTIR results of *B. coagulans* (ATCC 7050) crude metabolite and ZnO NPs. (C) XRD. (D) Zeta analysis. (E) TEM. Bars scale = 100 nm (E).

ZnO NPs had a surface positive charge equal to 29±2 mV according to Zeta potential test (Figure 2D). The TEM micrograph showed the good dispersion of the biosynthesized spherical-shaped ZnO NPs (Figure 2E). Also, the spherical shaped ZnO NPs with 5.40 - 6.79 nm range were demonstrated using *B. foraminis* as demonstrated by **EL-Ghwas (2022)**. While *B. subtilis* ZBP4 biosynthesized ZnO NPs with irregular spherical shape and size range of 22–59 nm as reported by **Hamk et al. (2022)**. The current results confirmed the high stability of the biosynthesized ZnO NPs due to the high repulsion forces between the particles due to its high surface positive charge values which prevent their aggregation and agglomeration. In addition, the FTIR results confirmed the presence of different proteins that will act as capping agents **(El-Dein et al., 2021)**.

A typical issue that reduces the biological potential of nanoparticles is the low stability and their tendency to aggregate. Capping agents were used to decrease and stop nanoparticles agglomeration and aggregation **(Duan et al., 2015)**. The existence of proteins as capping agents for ZnO NPs was confirmed by the FTIR spectrum and may also act as stabilising agents. Additionally, **Siddique et al. (2013)** speculate that charged nanoparticles may strengthen the attraction between particles, reducing the likelihood of particle aggregation. The biosynthesized ZnO NPs had a positive potential reached to 29±2 mV which produce strong repulsion force between the particles preventing its aggregation. Also, TEM micrograph showed the homogeneity of the biosynthesized ZnO NPs moreover their monodispersity in size.

Antimicrobial activity of biosynthesized ZnO NPs

Antimicrobial activity results showed that ZnO NPs were effective against both Gram-positive and Gram-negative bacteria as well as yeast (Figure 3). It was found that ZnO NPs showed higher antibacterial potential against the Gram-positive than Gram-negative bacteria due to the difference in their cell wall composition **(Balraj et al., 2017)**. Gram-positive bacterial cell wall contains high amounts of peptidoglycan and acidic components that strongly bind with the positively charged ZnO NPs which might increase their antibacterial action **(El-Zahed et al., 2022b)**. The presented results agree with **Premanathan et al. (2011)** findings. In addition, ZnO NPs showed antifungal action against one of the highest virulent pathogenic yeasts; *C. albicans*. The antimicrobial activity including antifungal action increased by increasing the concentration of ZnO NPs. 5000 µg/ml of ZnO NPs revealed an inhibition zone equal to 1.5 mm against *C. albicans* as reported by **Sharma & Ghose (2015)**. While **Janaki et al. (2015)** found that ZnO NPs showed inhibition zones (7, 8, 9, 9 and 10 mm) increases with increasing concentrations (62.5, 125, 250, 500 and 1000 µg/ml, respectively).

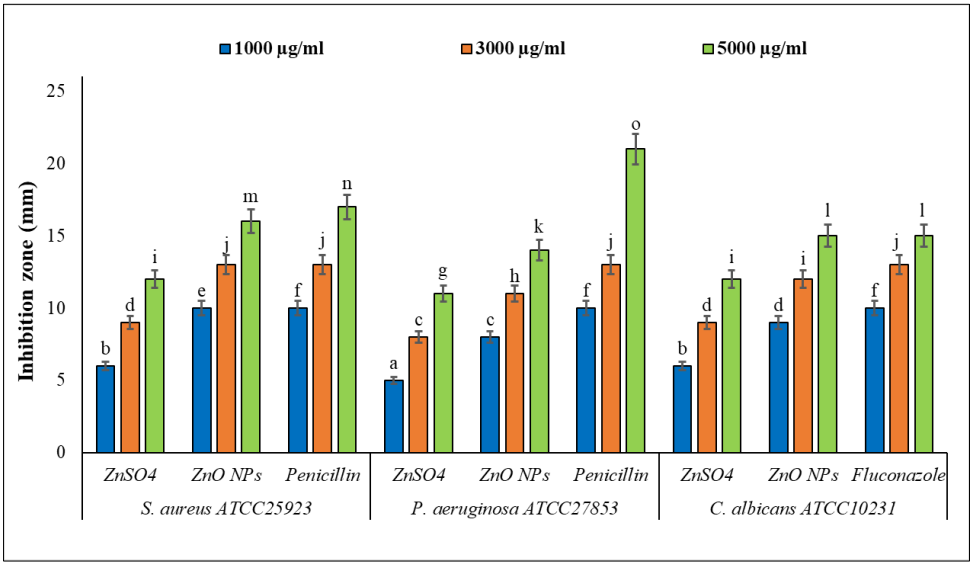

Figure 3 Antimicrobial activity of ZnO NPs comparing to other antimicrobial agents (1000, 3000 and 5000 µg/ml) against *S. aureus* ATCC 25923, *P. aeruginosa* ATCC 27853 and *C. albicans* ATCC 10231. Each column represents the mean of three replicates ± SE. Columns with common letters are not significantly different at $P < 0.05$.

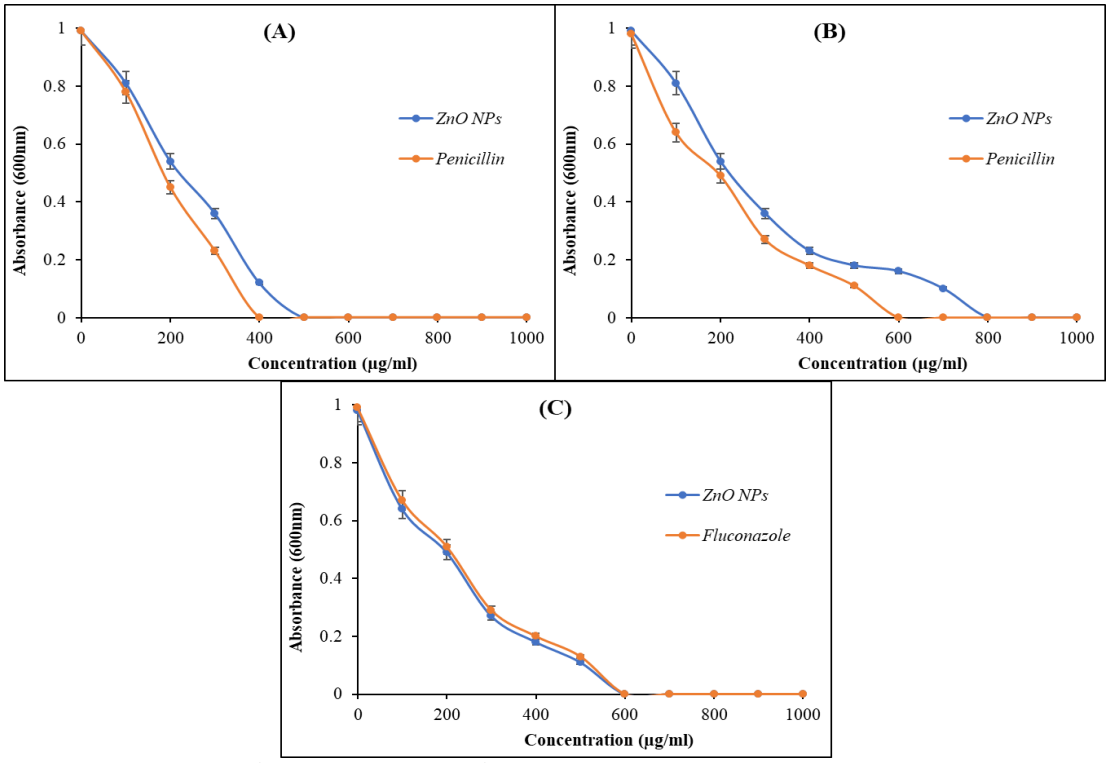

Figure 4 Minimum inhibition concentration of ZnO NPs, penicillin and fluconazole against *S. aureus* ATCC 25923; (A), *P. aeruginosa* ATCC 27853; (B), and *C. albicans* ATCC 10231; (C).

The MIC and MBC values of ZnO NPs in the current study were 800 and 900 µg/ml for *P. aeruginosa*, 500 and 700 µg/ml for *S. aureus* and 600 and 700 µg/ml for *C. albicans*, respectively showing a dose-related inhibitory effect (Figure 4). ZnO NPs revealed moderate to strong antibacterial activity compared to the standard antibacterial drug (penicillin). **Rehman et al. (2019)** recorded the MIC values of ZnO NPs against *E. coli* and *S. aureus* as >8000 and 4000 µg/ml, respectively. ZnO NPs showed anticandidal action similar to the reference drug (fluconazole) which recommended it as a potent anticandidal agent. On the other hand, ZnO NPs showed antifungal activity against *C. albicans* with an MIC of 5000 µg/ml as reported by **Gondal et al. (2012)**.

Ultrastructure of ZnO NPs-treated bacteria

The ZnO NPs impact on the ultrastructure of *P. aeruginosa* was assessed by TEM examination (Figure 5). Control bacterial cells had a smooth rod-shaped cell membrane and homogeneous cytoplasm. In contrast, ZnO NPs-treated bacterial cells showed irregular shapes and distinct morphological changes on the cell surface (Figure 5B). The malformation of the treated cells resulted in total cell lysis, release of cytoplasmic material, formation of lipids, separation of the outer membrane from the plasma membrane, and total loss of cytoplasm. Although the precise ZnO NPs antimicrobial mechanism is still unknown, some reported hypotheses suggested that ZnO NPs might interact with cellular proteins in cell membranes, attacking respiration and cell division and ultimately killing cells. In addition, the bactericidal effects of ZnO NPs were reported in different studies including formation of reactive oxygen species, cell wall damage and injuries in membrane permeability **(Sirelkhatim et al., 2015)**. The antimicrobial mechanism of ZnO NPs might be clarified through further studies.

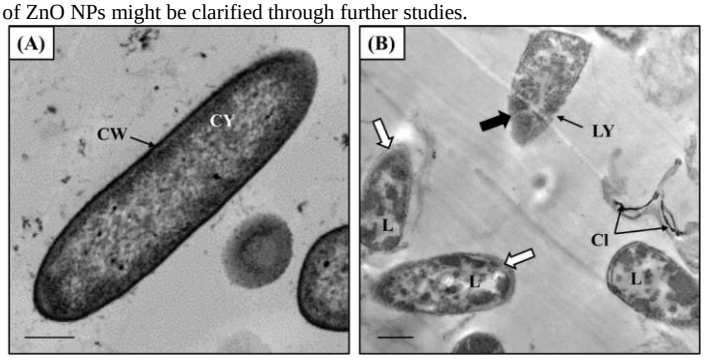

Figure 5 The bactericidal effect of ZnO NPs on the ultrastructure of *P. aeruginosa* ATCC 27853. A) Negative untreated controls (without ZnONPs) showed normal cell structure including cell wall (CW) and cytoplasm (CY). B) Treated bacterial samples (at MIC values) showed a separation between cell wall and cytoplasmic membrane (white arrows) with lysed cell walls (Ly), and complete cell lysis (Cl). Note the malformation of the treated cells (thick black arrow) with irregular shapes and lipids (L) formation.

Electrochemical studies of cell-free supernatants of ZnO NPs/*B. coagulans*

Regarding the use of bacteria in electrical current production, this refers to a process known as microbial electrochemical systems (MES). In an MES, microorganisms are used as biocatalysts to convert organic matter into electrical current. The use of harmful bacteria in an MES is common and can be beneficial because they can break down complex organic matter that other microorganisms cannot, thus increasing the efficiency of the system. However, it is important to note that the use of harmful bacteria in an MES requires careful consideration of safety and environmental impact. The current study demonstrated the use of the beneficial probiotic *B. coagulans* (ATCC 7050) as a new MES. Furthermore, *B. coagulans* can also reduce the need for costly pre-treatment of wastewater before it enters the MES **(Parihar et al., 2018; Singh et al., 2017)**.

ZnO NPs/*B. coagulans* metabolites produced high power density. To have a better knowledge of the electrochemical process at electrodes/solution interface and inside the solution, EIS Analyses were performed on two identical platinum electrodes with solution in between. Figure 6 illustrates current density-voltage and power density of *B. coagulans*. The power density curve was designed to examine voltage where power density as a function of current density. Short circuit current density is -0.0012 A.cm^{-2} which negative sign refers to output electricity and open circuit voltage is 0.335 V. Maximum value of power density 0.113 mW. cm^{-2}. The produced electricity is without external influences or catalyst factor, and this is attributed to the movement of ions inside the cell **(Marshall & May, 2009)**.

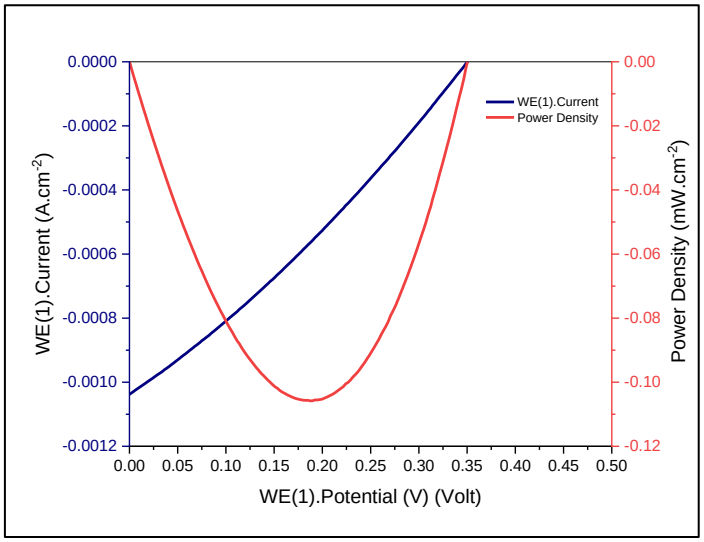

Figure 6 Current density–voltage characteristic and power density generated from ZnO NPs/*B. coagulans* metabolites.

Figure 7 shows EIS Nyquist plot Pt dummy cells whereas series resistance is 12.19 Ω.cm^2, Q = 1.244e-3 F.s^(a - 1), n= 0.644 4, R_{re} = 493.3 Ω.cm^2, and C_{ch}= 950.15e-6 F from these data we calculated ion conductivity (σ= 0.164 Ω^{-1}.cm^{-1}). On the other hand, Figure 8 illustrates EIS Nyquist plot Cu dummy cells whereas series resistance is 17.59 Ω.cm^2, Q = 1.24e-3 F.s^(a - 1), n= 0.751 6, R_{re} = 256.3Ω.cm^2, and C_{ch}= 847.93e-6 F from these data we calculated ion conductivity (σ= 0.113 Ω^{-1}.cm^{-1}). Figure 8 Shows output power density from ZnO NPs/*B. coagulans* metabolites. EIS analysis was carried out for two (dummy) Pt electrodes and identical electrodes of Cu with ZnO NPs/*B. coagulans* metabolites in between two electrodes. The primary goal of EIS analysis was to comprehend the behavior of ions at interface *B. coagulans*/electrode. There are critical parameters (chemical capacitor (C_{ch}), the recombination resistance (R_{re}), constant phase element (Q), constant phase (n), and series resistance (R_s) that are calculated from EIS analysis to understand ions performance in cell at electrodes. These parameters are computed using a proper equivalent circuit to fit the experimental data (R_s +Q1/(R_{re} +W2)).

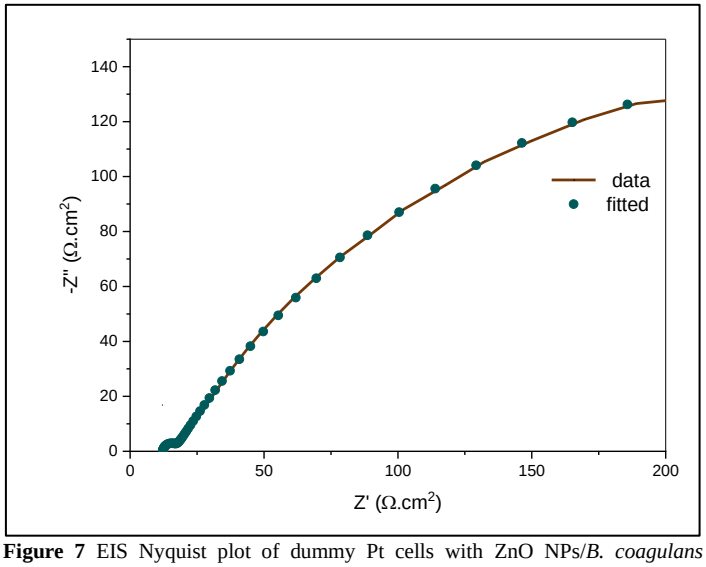

Figure 7 EIS Nyquist plot of dummy Pt cells with ZnO NPs/*B. coagulans* metabolites.

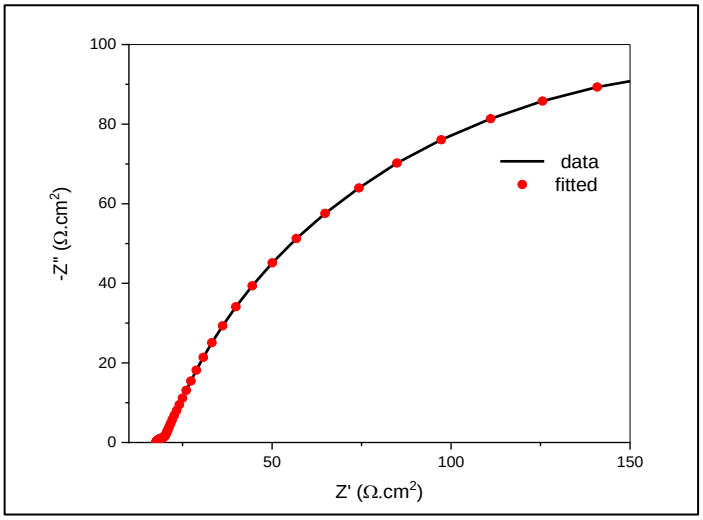

Figure 8 EIS Nyquist plot of dummy Cu cells with ZnO NPs/*B. coagulans* metabolites.

B. coagulans had a specific pathway to reduced nitrate (NO_3^-) into nitrite (NO_2^-) using extracellular NR which might produce the current. The bacterial total protein concentration (1277.6 ± 0.03 µg/ml) of *B. coagulans* was estimated by plotting of standard curve for bovine serum albumin protein sample with different known concentrations against absorbance values, the unknown samples were determined directly from the equation derived from the curve. The activity of NR was measured and calculated in the *B. coagulans* crude metabolite, at the rate of 2.18 U/ml. In addition, *B. coagulans* may transport electrons through their chemical compounds that found in its secondary metabolites into the environment as tiny currents which could assisted by ubiquitous flavin molecules enhancing electrons flowing into the electrodes **(Paquete, 2020)**. Although work on MES-capable bacteria is still in its early phases and the majority of applications are still in the development stage, there is great potential for making important advances in the field.

CONCLUSIONS

Zinc oxide nanoparticles (ZnO NPs) were biosynthesized using the cell-free bacterial supernatant of *Bacillus coagulans* (ATCC 7050). The provided biosynthesis approach was rapid, simple, cheap, and eco-friendly with high stability. To the best of our knowledge, this is the first report on the study of *B. coagulans* for biosynthesis of ZnO. The biosynthesized nanoparticles had higher biocidal activity against Gram-positive than Gram-negative bacteria moreover their strong antifungal action against *Candida albicans*. ZnO NPs/*B. coagulans* metabolites had high current value (voltage value ≈ >0.34 volt) which was enough to light a LED lamp as a new microbial electrochemical system (MES). The obtained results are considered as promising results for an applicable, cheap, renewable, and safe source of energy, especially in the field of electricity moreover their strong microbicidal action.

REFERENCES

Alarifi, S., Ali, D., Alkahtani, S., Verma, A., Ahamed, M., Ahmed, M., & Alhadlaq, H. A. (2013). Induction of oxidative stress, DNA damage, and apoptosis in a malignant human skin melanoma cell line after exposure to zinc oxide nanoparticles. *Int. J. Nanomedicine, 8,* 983–993. https://doi.org/10.2147/IJN.S42028

Azimirad, R., & Safa, S. (2014). Photocatalytic and antifungal activity of flower-like copper oxide nanostructures. *Synth. React. Inorganic, Met. Nano-Metal Chem.*, 44(6), 798–803. https://doi.org/10.1080/15533174.2013.790440

Balraj, B., Senthilkumar, N., Siva, C., Krithikadevi, R., Julie, A., Potheher, I. V., & Arulmozhi, M. (2017). Synthesis and characterization of zinc oxide nanoparticles using marine *Streptomyces* sp. with its investigations on anticancer and antibacterial activity. *Res. Chem. Intermed., 43(4),* 2367–2376. https://doi.org/10.1007/s11164-016-2766-6

Bradford, M. M. (1976). A rapid and sensitive method for the quantitation of microgram quantities of protein utilizing the principle of protein-dye binding. *Anal. Biochem., 72(1–2),* 248–254. https://doi.org/10.1016/0003-2697(76)90527-3

Clinical and Laboratory Standards. (2000). Methods for dilution antimicrobial susceptibility test for bacteria that grow aerobically. Wayne, PA Clin. Lab. Stand. Inst.

Clinical and Laboratory Standards. (2017). Performance standards for antimicrobial susceptibility testing. In Performance standards for antimicrobial susceptibility testing: Approved standard- twenty-seven Edition, Clinical and Laboratory Standards Institute. Clinical and Laboratory Standards Institute Wayne, PA.

Dizaj, S. M., Lotfipour, F., Barzegar-Jalali, M., Zarrintan, M. H., & Adibkia, K. (2014). Antimicrobial activity of the metals and metal oxide nanoparticles. *Mater. Sci. Eng. C, 44,* 278–284. https://doi.org/10.1016/j.msec.2014.08.031

Duan, H., Wang, D., & Li, Y. (2015). Green chemistry for nanoparticle synthesis. *Chem. Soc. Rev., 44(16),* 5778–5792. https://doi.org/10.1039/C4CS00363B

El-Dein, M. M. N., Baka, Z. A. M., Abou-Dobara, M. I., El-Sayed, A. K. A., & El-Zahed, M. M. (2021). Extracellular biosynthesis, optimization, characterization and antimicrobial potential of *Escherichia coli* D8 silver nanoparticles. *J. Microbiol. Biotechnol. Food Sci., 10(4),* 648–656. https://doi.org/10.15414/jmbfs.2021.10.4.648-656

EL-Ghwas, D. E. (2022). Characterization and biological synthesis of zinc oxide nanoparticles by new strain of *Bacillus foraminis*. *Biodiversitas J. Biol. Divers., 23(1).* https://doi.org/10.13057/biodiv/d230159

El-Nahhal, I. M., Elmanama, A. A., El Ashgar, N. M., Amara, N., Selmane, M., & Chehimi, M. M. (2017). Stabilization of nano-structured ZnO particles onto the surface of cotton fibers using different surfactants and their antimicrobial activity. *Ultrason. Sonochem., 38,* 478–487. https://doi.org/10.1016/j.ultsonch.2017.03.050

El-Zahed, M. M., Abou-Dobara, M. I., El-Sayed, A. K. A., & Baka, Z. A. M. (2022). Ag/SiO_2 nanocomposite mediated by *Escherichia coli* D8 and their antimicrobial potential. *Nov. Biotechnol. Chim., 21,* e1023. https://doi.org/10.36547/nbc.1023

El-Zahed, M. M., Baka, Z. A. M., El-Sayed, A. K. A., & Abou-Dobara, M. I. (2022). The anti-*Aspergillus* potential of optimized biosynthesized reduced graphene oxide/silver nanocomposite using *Escherichia coli* D8 (MF062579). *J. Microbiol. Biotechnol. Food Sci., 12(2),* e5864. https://doi.org/10.55251/jmbfs.5864

Faizan, M., Ahmed, R., & Ali, H. M. (2021). A critical review on thermophysical and electrochemical properties of ionanofluids (nanoparticles dispersed in ionic liquids) and their applications. *J. Taiwan Inst. Chem. Eng., 124,* 391–423. https://doi.org/https://doi.org/10.1016/j.jtice.2021.02.004

Gold, K., Slay, B., Knackstedt, M., & Gaharwar, A. K. (2018). Antimicrobial activity of metal and metal-oxide based nanoparticles. *Adv. Ther., 1(3),* 1700033. https://doi.org/https://doi.org/10.1002/adtp.201700033

Gondal, M. A., Alzahrani, A. J., Randhawa, M. A., & Siddiqui, M. N. (2012). Morphology and antifungal effect of nano-ZnO and nano-Pd-doped nano-ZnO against *Aspergillus* and *Candida*. *J. Environ. Sci. Heal. Part A, 47(10),* 1413–1418. https://doi.org/10.1080/10934529.2012.672384

Griffith, A., Mateen, A., Markowitz, K., Singer, S. R., Cugini, C., Shimizu, E., Wiedman, G. R., & Kumar, V. (2022). Alternative antibiotics in dentistry: Antimicrobial peptides. *Pharmaceutics, 14(8),* 1679. https://doi.org/10.3390/pharmaceutics14081679

Hamk, M., Akçay, F. A., & Avcı, A. (2022). Green synthesis of zinc oxide nanoparticles using *Bacillus subtilis* ZBP4 and their antibacterial potential against foodborne pathogens. *Prep. Biochem. Biotechnol.*, 1–10. https://doi.org/10.1080/10826068.2022.2076243

Harley, S. M. (1993). Use of a simple, colorimetric assay to demonstrate conditions for induction of nitrate reductase in plants. *Am. Biol. Teach., 55(3),* 162–164. https://doi.org/10.2307/4449615

Hazra, M., Joshi, H., Williams, J. B., & Watts, J. E. M. (2022). Antibiotics and antibiotic resistant bacteria/genes in urban wastewater: A comparison of their fate in conventional treatment systems and constructed wetlands. *Chemosphere, 303,* 135148. https://doi.org/10.1016/j.chemosphere.2022.135148

Jagadeeshan, S., & Parsanathan, R. (2019). Nano-metal oxides for antibacterial activity. In Advanced Nanostructured Materials for Environmental Remediation (pp. 59–90). Springer. https://doi.org/10.1007/978-3-030-04477-0_3

Janaki, A. C., Sailatha, E., & Gunasekaran, S. (2015). Synthesis, characteristics and antimicrobial activity of ZnO nanoparticles. *Spectrochim. Acta Part A Mol. Biomol. Spectrosc., 144,* 17–22. https://doi.org/10.1016/j.saa.2015.02.041

Karimiyan, A., Najafzadeh, H., Ghorbanpour, M., & Hekmati-Moghaddam, S. H. (2015). Antifungal effect of magnesium oxide, zinc oxide, silicon oxide and copper oxide nanoparticles against *Candida albicans*. *Zahedan J. Res. Med. Sci., 17(10).* https://doi.org/10.17795/zjrms-2179

Khan, F. A. (2020). Synthesis of nanomaterials: methods & technology. In Applications of Nanomaterials in Human Health (pp. 15–21). Springer. https://doi.org/10.1007/978-981-15-4802-4_2

Khurana, C., Vala, A. K., Andhariya, N., Pandey, O. P., & Chudasama, B. (2014). Antibacterial activity of silver: The role of hydrodynamic particle size at nanoscale. *J. Biomed. Mater. Res. Part A, 102(10),* 3361–3368. https://doi.org/10.1002/jbm.a.35005

Lai, Y., Meng, M., Yu, Y., Wang, X., & Ding, T. (2011). Photoluminescence and photocatalysis of the flower-like nano-ZnO photocatalysts prepared by a facile hydrothermal method with or without ultrasonic assistance. *Appl. Catal. B Environ., 105(3–4),* 335–345. https://doi.org/10.1016/j.apcatb.2011.04.028

Lisha, L., Mousa, S., Arnone, G., Muda, I., Huerta-Soto, R., & Shiming, Z. (2023). Natural resources, green innovation, fintech, and sustainability: A fresh insight from BRICS. *Resour. Policy, 80,* 103119. https://doi.org/10.1016/j.resourpol.2022.103119

Liu, Y., Tran, D. Q., & Rhoads, J. M. (2018). Probiotics in disease prevention and treatment. *J. Clin. Pharmacol., 58,* S164–S179. https://doi.org/10.1002/jcph.1121

Lovley, D. R., & Phillips, E. J. P. (1988). Novel mode of microbial energy metabolism: organic carbon oxidation coupled to dissimilatory reduction of iron or manganese. *Appl. Environ. Microbiol., 54(6),* 1472–1480. https://doi.org/10.1128/aem.54.6.1472-1480.1988

Mahdi, Z. S., Talebnia Roshan, F., Nikzad, M., & Ezoji, H. (2021). Biosynthesis of zinc oxide nanoparticles using bacteria: A study on the characterization and application for electrochemical determination of bisphenol A. *Inorg. Nano-Metal Chem., 51(9),* 1249–1257. https://doi.org/10.1080/24701556.2020.1835962

Malvankar, N. S., Vargas, M., Nevin, K. P., Franks, A. E., Leang, C., Kim, B.-C., Inoue, K., Mester, T., Covalla, S. F., & Johnson, J. P. (2011). Tunable metallic-like conductivity in microbial nanowire networks. *Nat. Nanotechnol., 6(9),* 573–579. https://doi.org/10.1038/nnano.2011.119

Mariotti, N., Bonomo, M., Fagiolari, L., Barbero, N., Gerbaldi, C., Bella, F., & Barolo, C. (2020). Recent advances in eco-friendly and cost-effective materials towards sustainable dye-sensitized solar cells. *Green Chem., 22(21),* 7168–7218. https://doi.org/10.1039/D0GC01148G

Marshall, C. W., & May, H. D. (2009). Electrochemical evidence of direct electrode reduction by a thermophilic Gram-positive bacterium, *Thermincola ferriacetica*. *Energy Environ. Sci., 2(6),* 699–705. https://doi.org/10.1039/B823237G

Mohd Yusof, H., Rahman, A., Mohamad, R., Zaidan, U. H., & Samsudin, A. A. (2020). Biosynthesis of zinc oxide nanoparticles by cell-biomass and supernatant of *Lactobacillus plantarum* TA4 and its antibacterial and biocompatibility properties. *Sci. Rep., 10(1),* 1–13. https://doi.org/10.1038/s41598-020-76402-w

Mousa, M. A., & Khairy, M. (2020). Synthesis of nano-zinc oxide with different morphologies and its application on fabrics for UV protection and microbe-resistant defense clothing. *Text. Res. J., 90(21–22),* 2492–2503. https://doi.org/10.1177/0040517520920952

Mukhaifi, E. A., & Abduljaleel, S. A. (2020). Electric bacteria: a review. *J. Adv. Lab. Res. Biol., 11(1),* 7–15.

O'connor, B. P. (2000). SPSS and SAS programs for determining the number of components using parallel analysis and Velicer's MAP test. *Behav. Res. Methods, Instruments, Comput., 32(3),* 396–402. https://doi.org/10.3758/BF03200807

Pandit, C., Roy, A., Ghotekar, S., Khusro, A., Islam, M. N., Emran, T. Bin, Lam, S. E., Khandaker, M. U., & Bradley, D. A. (2022). Biological agents for synthesis of nanoparticles and their applications. *J. King Saud Univ., 34(3),* 101869. https://doi.org/10.1016/j.jksus.2022.101869

Paquete, C. M. (2020). Electroactivity across the cell wall of Gram-positive bacteria. *Comput. Struct. Biotechnol. J., 18,* 3796–3802. https://doi.org/10.1016/j.csbj.2020.11.021

Parihar, V., Raja, M., & Paulose, R. (2018). A brief review of structural, electrical and electrochemical properties of zinc oxide nanoparticles. *Rev. Adv. Mater. Sci., 53(2),* 119–130.. https://doi.org/10.1515/rams-2018-0009

Premanathan, M., Karthikeyan, K., Jeyasubramanian, K., & Manivannan, G. (2011). Selective toxicity of ZnO nanoparticles toward Gram-positive bacteria and cancer cells by apoptosis through lipid peroxidation. *Nanomedicine Nanotechnology, Biol. Med., 7(2),* 184–192. https://doi.org/10.1016/j.nano.2010.10.001

Raina, S., Roy, A., & Bharadvaja, N. (2020). Degradation of dyes using biologically synthesized silver and copper nanoparticles. *Environ. Nanotechnology, Monit. Manag., 13,* 100278. https://doi.org/https://doi.org/10.1016/j.enmm.2019.100278

Rajabairavi, N., Raju, C. S., Karthikeyan, C., Varutharaju, K., Nethaji, S., Hameed, A. S. H., & Shajahan, A. (2017). Biosynthesis of novel zinc oxide nanoparticles (ZnO NPs) using endophytic bacteria *Sphingobacterium thalpophilum*. In Recent trends in materials science and applications (pp. 245–254). Springer. https://doi.org/10.1007/978-3-319-44890-9_23

Rajput, N. (2015). Methods of preparation of nanoparticles-a review. *Int. J. Adv. Eng. Technol., 7(6),* 1806.

Raval, J., Trivedi, R., Suman, S., Kukrety, A., & Prajapati, P. (2022). Nano-biotechnology and its innovative perspective in diabetes management. *Mini Rev. Med. Chem., 22(1),* 89–114. https://doi.org/10.2174/1389557521666210623164052

Rehman, S., Jermy, B. R., Akhtar, S., Borgio, J. F., Abdul Azeez, S., Ravinayagam, V., Al Jindan, R., Alsalem, Z. H., Buhameid, A., & Gani, A. (2019). Isolation and characterization of a novel thermophile; *Bacillus haynesii*, applied for the green synthesis of ZnO nanoparticles. *Artif. Cells, Nanomedicine, Biotechnol., 47(1),* 2072–2082. https://doi.org/10.1080/21691401.2019.1620254

Sharma, R. K., & Ghose, R. (2015). Synthesis of zinc oxide nanoparticles by homogeneous precipitation method and its application in antifungal activity against *Candida albicans*. *Ceram. Int., 41(1, Part B),* 967–975. https://doi.org/j.ceramint.2014.09.016

Shivashankarappa, A., & Sanjay, K. R. (2015). Study on biological synthesis of cadmium sulfide nanoparticles by *Bacillus licheniformis* and its antimicrobial properties against food borne pathogens. *Nanosci Nanotechnol Res, 3(1),* 6–15. https://doi.org/10.12691/nnr-3-1-2

Siddique, Y. H., Fatima, A., Jyoti, S., Naz, F., Rahul, Khan, W., Singh, B. R., & Naqvi, A. H. (2013). Evaluation of the toxic potential of graphene copper nanocomposite (GCNC) in the third instar larvae of transgenic *Drosophila melanogaster* (hsp70-lacZ)Bg9. *PLoS One, 8(12),* e80944. https://doi.org/10.1371/journal.pone.0080944

Singh, S., Joshi, M., Panthari, P., Malhotra, B., Kharkwal, A. C., & Kharkwal, H. (2017). Citrulline rich structurally stable zinc oxide nanostructures for superior photo catalytic and optoelectronic applications: A green synthesis approach. *Nano-Structures & Nano-Objects, 11,* 1–6. https://doi.org/10.1016/j.nanoso.2017.05.006

Sirelkhatim, A., Mahmud, S., Seeni, A., Kaus, N. H. M., Ann, L. C., Bakhori, S. K. M., Hasan, H., & Mohamad, D. (2015). Review on zinc oxide nanoparticles: Antibacterial activity and toxicity mechanism. *Nano-Micro Lett., 7(3),* 219–242. https://doi.org/10.1007/s40820-015-0040-x

Thareja, S., & Kumar, A. (2021). *In Situ* wet synthesis of N-ZnO/N-rGO nanohybrids as an electrode material for high-performance supercapacitors and simultaneous nonenzymatic electrochemical sensing of ascorbic acid, dopamine, and uric acid at their interface. *J. Phys. Chem. C, 125(45),* 24837–24848. https://doi.org/10.1021/acs.jpcc.1c08413

Yin, I. X., Zhang, J., Zhao, I. S., Mei, M. L., Li, Q., & Chu, C. H. (2020). The antibacterial mechanism of silver nanoparticles and its application in dentistry. *Int. J. Nanomedicine, 15,* 2555–2562. https://doi.org/10.2147/IJN.S246764

Yu, K.-P., Huang, Y.-T., & Yang, S.-C. (2013). The antifungal efficacy of nano-metals supported TiO_2 and Ozone on the resistant *Aspergillus niger* spore. *J. Hazard. Mater., 261,* 155–162. https://doi.org/10.1016/j.jhazmat.2013.07.029

Yusof, H. M., Mohamad, R., Zaidan, U. H., & Abdul Rahman, N. A. (2019). Microbial synthesis of zinc oxide nanoparticles and their potential application as an antimicrobial agent and a feed supplement in animal industry: A review. *J. Anim. Sci. Biotechnol., 10(1),* 57. https://doi.org/10.1186/s40104-019-0368-z

Zhang, H., Wang, Y., Zhao, W., Zou, M., Chen, Y., Yang, L., Xu, L., Wu, H., & Cao, A. (2017). MOF-derived ZnO nanoparticles covered by N-doped carbon layers and hybridized on carbon nanotubes for lithium-ion battery anodes. *ACS Appl. Mater. Interfaces, 9(43),* 37813–37822. https://doi.org/10.1021/acsami.7b12095

Zhao, L., Lu, L., Wang, A., Zhang, H., Huang, M., Wu, H., Xing, B., Wang, Z., & Ji, R. (2020). Nano-biotechnology in agriculture: use of nanomaterials to promote plant growth and stress tolerance. *J. Agric. Food Chem., 68(7),* 1935–1947. https://doi.org/10.1021/acs.jafc.9b06615